

Article

Surface Waves on a Coated Homogeneous Half-Space under the Effects of External Forces

Ali M. Mubaraki * and Fadhel M. Almalki

Department of Mathematics and Statistics, College of Science, Taif University, P.O. Box 11099, Taif 21944, Saudi Arabia

* Correspondence: alimobarki@tu.edu.sa

Abstract: The present study focuses on the examination of the propagation of plane surface waves on a coated half-space, which is accompanied by the magnetic field force, and the normal mechanical loading, due to Winkler's elastic foundation. The study is based upon the application of the analytical and asymptotic integration procedures to acquire and further analyze the aspiring secular equation. Asymptotically, the influence of the coating layer is suppressed by deploying apposite effective boundary conditions that are ingrained on a long-wave approximation condition, to obtain the resulting pseudo-differential operator of the reduced equation of surface motion. In fact, the comparison between the two approaches yielded considerable agreement through the dependency plots, featuring the scaled velocity v/v_R versus the dimensionless wavenumber K . Moreover, certain well-known results in the literature are obtained as limiting circumstances of the present examination. Additionally, an insightful finding about the vanishing possibility of the coating layer is illustratively highlighted.

Keywords: surface waves; coated half-space; magnetic field force; Winkler's elastic foundation



Citation: Mubaraki, A.M.; Almalki, F.M. Surface Waves on a Coated Homogeneous Half-Space under the Effects of External Forces. *Symmetry* **2022**, *14*, 2241. <https://doi.org/10.3390/sym14112241>

Academic Editor: Jan Awrejcewicz

Received: 7 October 2022

Accepted: 20 October 2022

Published: 25 October 2022

Publisher's Note: MDPI stays neutral with regard to jurisdictional claims in published maps and institutional affiliations.



Copyright: © 2022 by the authors. Licensee MDPI, Basel, Switzerland. This article is an open access article distributed under the terms and conditions of the Creative Commons Attribution (CC BY) license (<https://creativecommons.org/licenses/by/4.0/>).

1. Introduction

Modern technological advancements in the areas of science and engineering application has resulted in the quest for coated and composites structures due to their various advantages and applications; the construction of medical biomaterials that improve the quality of life is, in particular, enough to see the imperativeness of the modeling and analysis of coated structures [1,2], in addition to their relevance in many engineering professions, including, for example, mechanical, aeronautics, civil, and manufacturing engineering to mention a few. We also recall their significance in material science, glazing and flooring, and above all, its applicability in the design and construction of the multi-layered media [3–7]. Moreover, the propagation of surface waves in coated elastic solids have inspired many research questions in recent times, having frequently arisen, for instance, in modeling seismic protection, improving highways and rail transportation quality to mention a few, see, for example, [8–14] and the references provided therein for more readings. The Rayleigh wave propagation, being a form of a surface wave on a homogeneous elastic half-space, is widely known to occur only for stress-free surfaces [15,16]. However, several investigations have recently been conducted on the impact of external factors that infiltrate or otherwise influence the propagation of surface waves in assorted media. The internal and external forces such as the gravitational force, magnetic field force, and damping force, to name a few, are known to influence the propagation of waves; one can also consider other well-known factors that significantly distort the propagation of elastic waves such as the external loads, e.g., elastic foundations, initial stress, rotational effects, porosity presence, material inhomogeneity, and cracks, among others, see [17–24] and the references listed therein for a quick review of such phenomena. Additionally, the thermal heating effect is equally a vital phenomenon with vast relevance in the field of elasticity, which later metamorphosed to the theory of thermo-elasticity [25–31].

However, within this work, we further expand on the considerations presented by Kaplunov et al. [8,10] by replicating an interesting scenario of a coated half-space substrate under the influence of certain external forces—modeling a interface between the rigid coating layer and deformable semi-infinite substrate. The major focus is on gaining a physical understanding of the characteristics of the localized dynamic phenomena amidst external forces by using an asymptotic approach [13]; read about the generalized asymptotic analysis method for seeking the contributions of edge, surface, and interfacial waves from the dynamic of external loads and different effects in [32–34]. Furthermore, in Kaplunov et al. [8], the significance of a thin coating covering a homogenous elastic half-space was tackled by deriving the corresponding effective boundary conditions down the surface of a semi-infinite half-space, having initially prescribed a clamped-surface condition on the upper face of the coating; whereas, Dai et al. [10] examined the long-wave propagation scenario of surface waves in a coated semi-infinite range with the stress-free end condition. Equally, both the low- and high-frequency vibrations were analyzed, in addition to the presentation of their asymptotic treatments of the higher-order Rayleigh-type waves with a periodic distinction in [8], one can also read similar studies related to the modeling and examination of elastic structures with thin layers and walls in [33,35,36]. However, in this regard, the idea for the construction of the associated effective boundary conditions, which is also analogous to the interfacial conditions for hyperbolic-elliptic formulation to study the Rayleigh-type waves which firstly appeared in the works of Kaplunov and Kossovich [37], with further advances in [33]. The same method was also used for various propagation problems in elastic media, including coated half-spaces [8–14], where a pseudo-differential operator is realized, and the crack propagation scenario related to the mixed boundary value problems [22]. More so, the method provides the asymptotic formulas for the corrections to the Rayleigh wave speed in favor of the thin light coating that follows from the pseudo-differential equation along the half-space surface.

In brief, the present research is aimed at modeling and analyzing the propagation of plane surface wave scenarios with regard to a half-space coated by a light-coating layer under the influence of certain external forces. However, since there are a number of external forces in the literature, we will be considering the structure under deliberation to be exposed to the magnetic field force [12] and the normal mechanical load due to Winkler’s elastic foundation [30,38,39] only, respectively, owing to their practical thoughts and natural occurrence. A methodology kit, comprising analytical and asymptotic tools, will be deployed, such that the influence of the coating layer is to be asymptotically tackled through the acquisition of apposite effective boundary conditions [10,13]—depending on the long-wave approximation condition [40]. Moreover, the presentation of the present paper takes the following outline: Section 2 presents the formulation, as well as the determination of the exact solution to the problem. Section 3 prescribes appropriate boundary and interfacial conditions for the coated half-space under deliberation, while Section 4 determines the generalized exact secular equation and its numerical illustration. Section 5 obtains an approximate secular equation asymptotically, while Section 6 provides a discussion on the vanishing effect of the coating layer, and Section 7 provides certain finishing notes.

2. Problem Formulation

Let us begin by considering the governing equations of motion under the influence of magnetic field force \vec{F}_i as follows [12,15,16]

$$\sigma_{ij,j} + \vec{F}_i = \rho_q u_{i,tt}, \quad (1)$$

where the magnetic force is expressed as follows [41]

$$\vec{F}_i = \mu_0 H_0^2 (e_{,1} - \epsilon_0 \mu_0 u_{1,tt}, e_{,2} - \epsilon_0 \mu_0 u_{2,tt}, 0), \quad (2)$$

with $e = u_{1,1} + u_{2,2}$. Further in the paper, we define all the terms involved.

Thus, the present study considers a coated elastic half-space that is subject to certain external forces, including the magnetic field force, and the normal mechanical load P acting along the surface of the coating layer. Here, both the coating and the half-space layers are assumed to be homogeneous, and are further supposed to be made of isotropic material. Moreover, the entire structure is then recognized to be an inhomogeneous structure in relation to the varying material properties in the layers. Additionally, the coating layer is presumed to have a constant thickness of h that occupies the interval $-h \leq x_2 \leq 0$, while the half-space layer is perfectly interfaced over the semi-infinite interval $0 \leq x_2 < \infty$. In addition, this scenario is illustrated in Figure 1.

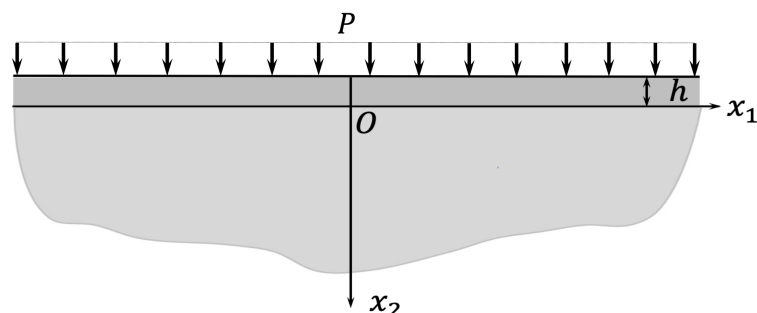


Figure 1. A coated homogeneous half-space under the effect of external forces.

More precisely, the two-dimensional (2D) dynamic equations of motion interoperating with the magnetic field force in the two isotropic homogeneous layers of the coated half-space are, respectively, given in component form from (1) and (2) as follows

$$\begin{aligned} \sigma_{11,1}^q + \sigma_{12,2}^q + \mu_0 H_0^2 (u_{1,11}^q + u_{2,21}^q - \epsilon_0 \mu_0 u_{1,tt}^q) &= \rho_q u_{1,tt}^q, \\ \sigma_{21,1}^q + \sigma_{22,2}^q + \mu_0 H_0^2 (u_{1,12}^q + u_{2,22}^q - \epsilon_0 \mu_0 u_{2,tt}^q) &= \rho_q u_{2,tt}^q, \end{aligned} \tag{3}$$

where σ_{ij}^q are the related stresses defined by

$$\sigma_{ij}^q = \lambda_q \epsilon_{kk}^q \delta_{ij} + 2\mu_q \epsilon_{ij}^q, \quad \epsilon_{ij}^q = \frac{1}{2} (u_{i,j}^q + u_{j,i}^q), \quad i = j = 1, 2, \tag{4}$$

with ϵ_{ij}^q denoting the strain–displacement relation, $u_1^q = u_1^q(x_1, x_2, t)$ and $u_2^q = u_2^q(x_1, x_2, t)$ are the in-plane displacements under consideration, δ_{ij} is the Kronecker delta, while ρ_q and μ_q, λ_q are the densities and the Lamé elastic constants in the respective regions of the coating and half-space, respectively, for $q = c, s$. Furthermore, the presence of the magnetic field force has resulted in the attendance of the magnetic field intensity H_0 , electric permeability ϵ_0 , and the magnetic permeability μ_0 .

Thus, upon expressing the above equations of dynamic equations of motion expressed in (3) in a component form, we now rewrite them in terms of displacements $u_j, (j = 1, 2)$ as follows

$$\begin{aligned} (\lambda_q + 2\mu_q + \mu_0 H_0^2) u_{1,11}^q + (\lambda_q + \mu_q + \mu_0 H_0^2) u_{2,12}^q + \mu_q u_{1,22}^q - (\rho_q + \epsilon_0 \mu_0^2 H_0^2) u_{1,tt}^q &= 0, \\ (\lambda_q + 2\mu_q + \mu_0 H_0^2) u_{2,22}^q + (\lambda_q + \mu_q + \mu_0 H_0^2) u_{1,12}^q + \mu_q u_{2,11}^q - (\rho_q + \epsilon_0 \mu_0^2 H_0^2) u_{2,tt}^q &= 0, \end{aligned} \tag{5}$$

for $q = c, s$.

The displacements $u_j^q, (j = 1, 2)$ can be expressed further through the following potential functions ϕ^q and ψ^q as follows [12]

$$u_1^q = \phi_{,1}^q - \psi_{,2}^q, \quad u_2^q = \phi_{,2}^q + \psi_{,1}^q, \tag{6}$$

which leads to the uncoupled equations of magneto-elastic wave motion

$$\phi_{,11}^q + \phi_{,22}^q - \frac{1}{v_{1q}^2} \phi_{,tt}^q = 0, \quad \psi_{,11}^q + \psi_{,22}^q - \frac{1}{v_{2q}^2} \psi_{,tt}^q = 0, \quad (7)$$

where v_{1q} and v_{2q} are the known longitudinal and transverse speeds in isotropic homogeneous magneto-elastic bodies, expressed explicitly as follows

$$v_{1q} = \sqrt{\frac{\lambda_q + 2\mu_q + H_0^2 \mu_0}{\rho_q + \mu_0^2 H_0^2 \varepsilon_0}}, \quad v_{2q} = \sqrt{\frac{\mu_q}{\rho_q + \mu_0^2 H_0^2 \varepsilon_0}}, \quad q = c, s. \quad (8)$$

Note, from the above speeds, in the absence of magnetic field force, that is, when $H_0 \rightarrow 0$, the respective speeds reduce accordingly to

$$v_{1q} = \sqrt{\frac{\lambda_q + 2\mu_q}{\rho_q}}, \quad v_{2q} = \sqrt{\frac{\mu_q}{\rho_q}}, \quad q = c, s, \quad (9)$$

which are the known respective longitudinal and transverse speeds of an isotropic homogeneous medium [32,40].

Hence, we further sought solutions for the un-coupled equations of magneto-elastic motion expressed in (7) via the supposed potentials functions ϕ^q and ψ^q as follows

$$\phi^q = f_{1q}(x_2) e^{ik(x_1 - vt)}, \quad \psi^q = f_{2q}(x_2) e^{ik(x_1 - vt)}, \quad (10)$$

where k and v are the dimensional wavenumber and the phase speed, respectively.

On introducing the solutions (10) into (7), we arrive at

$$f_{1q,22} - k^2 \alpha_q^2 f_{1q} = 0, \quad f_{2q,22} - k^2 \beta_q^2 f_{2q} = 0, \quad (11)$$

where α_q and β_q ($q = c, s$) are defined as

$$\alpha_q = \sqrt{1 - \frac{v^2}{v_{1q}^2}}, \quad \text{and} \quad \beta_q = \sqrt{1 - \frac{v^2}{v_{2q}^2}}. \quad (12)$$

Therefore, the solution of (7) via (10) and (11) may be given for the coating layer as

$$\phi^c = (A_{1c} e^{k\alpha_c x_2} + A_{2c} e^{-k\alpha_c x_2}) e^{ik(x_1 - vt)}, \quad \psi^c = (A_{3c} e^{k\beta_c x_2} + A_{4c} e^{-k\beta_c x_2}) e^{ik(x_1 - vt)}, \quad (13)$$

while, for the half-space layer that decays away from the surface $x_2 = 0$, its solution may be expressed in the following pattern

$$\phi^s = A_{1s} e^{-k\alpha_s x_2} e^{ik(x_1 - vt)}, \quad \psi^s = A_{2s} e^{-k\beta_s x_2} e^{ik(x_1 - vt)}, \quad (14)$$

where A_{1c} , A_{2c} , A_{3c} , A_{4c} , A_{1s} , and A_{2s} arising from (13) and (14) are constants to be determined later.

3. Boundary Conditions

The imposed boundary conditions under the external forces at the surface $x_2 = -h$ are given as

$$\sigma_{12}^c + \tau_{12}^c = 0, \quad \text{and} \quad \sigma_{22}^c + \tau_{22}^c = -P, \quad j = 1, 2, \quad (15)$$

where $P = P(x_1, t)$ in the last equation is a normal mechanical load that is considered to be due to an elastic Winkler foundation, which is further expressed as [30,38,39]

$$P = p u_2^c |_{x_2 = -h}, \quad (16)$$

where p is the dimensional stiffness of Winkler's elastic foundation. Furthermore, the stresses σ_{j2}^q and τ_{j2}^q for $j = 1, 2$, and $q = c, s$ are the mechanical stresses and Maxwell's stresses caused by the presence of a magnetic field force, respectively.

In addition, the following interfacial conditions between the coating and the half-space layers at $x_2 = 0$ are obtained as

$$u_j^c = u_j^s, \quad \text{and} \quad \sigma_{j2}^c + \tau_{j2}^c = \sigma_{j2}^s + \tau_{j2}^s, \quad j = 1, 2. \quad (17)$$

Moreover, the Maxwell's stresses τ_{j2}^q caused by the presence of a magnetic field force, are further considered to have the following tensorial representation

$$\tau_{ij}^q = \mu_0 H_0 \left(H_i^q h_j^q + H_j^q h_i^q - H_k^q h_k^q \delta_{ij} \right), \quad i = j = 1, 2, \quad q = c, s, \quad (18)$$

such that the corresponding normal and tangential stresses take the following explicit linearized forms

$$\tau_{22}^q = \mu_0 H_0^2 \left(u_{1,1}^q + u_{2,2}^q \right), \quad \text{and} \quad \tau_{12}^q = 0, \quad q = c, s. \quad (19)$$

Additionally, in the above equations, H_i^q is the magnetic field vector that takes the following definition

$$H_i^q = (h_i^q + H_0) \delta_{i2}, \quad i = 1, 2, \quad q = c, s. \quad (20)$$

with δ_{ij} representing the Kronecker delta taking the values in $\{0, 1\}$, while $H_0 = (0, 0, H_0)$ denotes the magnetic field intensity, which is taken along the x_3 direction—with the structure reclining over the $x_1 x_2$ plane. Additionally, h_i^q represents the perturbed magnetic field upon which it takes Einstein's summation form [12,16]

$$h_i^q = -u_{k,k}^q, \quad j = k = 1, 2, \quad q = c, s. \quad (21)$$

Note that we assume the magnetic field parameters to be the same in both layers, for the sake of simplicity.

4. Secular Equation and Numerical Illustrations

Deploying the expressions expressed in Equations (13) and (14) into the boundary and continuity conditions prescribed in (17) and (19), we obtain a homogeneous system of order six with the non-zero components. The dispersion relation, or rather, the secular equation, is then obtained as follows:

$$\text{Det} \left[\begin{pmatrix} i\alpha_c e^{-\alpha_c K} & -i\alpha_c e^{\alpha_c K} & -\delta_c^2 e^{-\beta_c K} & -\delta_c^2 e^{\beta_c K} & 0 & 0 \\ \chi_1^+ e^{-\alpha_c K} & \chi_1^- e^{\alpha_c K} & i\chi_2^+ e^{-\beta_c K} & -i\chi_2^- e^{\beta_c K} & 0 & 0 \\ i & i & -\beta_c & \beta_c & -i & -\beta_s \\ \alpha_c & -\alpha_c & i & i & \alpha_s & -i \\ i\mu \alpha_c & -i\mu \alpha_c & -\mu \delta_c^2 & -\mu \delta_c^2 & i\alpha_s & \delta_s^2 \\ \mu \delta_c^2 & \mu \delta_c^2 & i\mu \beta_c & -i\mu \beta_c & -\delta_s^2 & i\beta_s \end{pmatrix} \right] = 0, \quad (22)$$

with

$$\chi_1^\pm = \delta_c^2 \pm \frac{\alpha_c \zeta}{2K}, \quad \chi_2^\pm = \beta_c \pm \frac{\alpha_c \zeta}{2K}, \quad \delta_q = \frac{1}{2} \left(1 + \beta_q^2 \right), \quad q = c, s, \quad (23)$$

where the dimensionless Lamé elastic constant μ , dimensionless wavenumber K , and the dimensionless stiffness of the Winkler's elastic foundation ζ , are respectively expressed as follows:

$$\mu = \frac{\mu_c}{\mu_s}, \quad K = kh, \quad \zeta = \frac{hp}{\mu_c}. \quad (24)$$

Moreover, it can be demonstrated that at $h = 0$, that is, when the the coating layer vanishes, the secular equation expressed in (22) corresponds to that of the half-space only, which then takes the following reduced version form

$$\left(1 + \beta_s^2\right)^2 - 4\alpha_s \beta_s = 0. \quad (25)$$

In fact, upon making use of the explicit expressions for α_s and β_s as expressed in (12), the very well known Rayleigh wave equation is achieved [12,15].

In addition, the numerical simulation and results of the governing model via the obtained secular equation in (22), are performed in the present study by considering the following physical data of much concern, considered interchangeably in both the coating and the half-space layers, as follows [42–44].

Furthermore, in Table 1, ρ stands for the density, E stands for Young's modulus, while ν is the Poisson ratio. Furthermore, in favor of the magnetic field force presence, we consider the following fixed values (unless otherwise stated) as follows [12].

$$\mu_0 = 4\pi \times 10^{-7} \text{ kg m s}^{-2} \text{ A}^{-2}, \quad \epsilon_0 = 8.85 \times 10^{-12} \text{ kg}^{-1} \text{ m}^{-3} \text{ s}^4 \text{ A}^2.$$

Numerical illustrations of the dispersion curves via the obtained secular equation in (22)—showing the relationship between the dimensionless phase speed v/v_R and the dimensionless wavenumber K —are presented in Figures 2 and 3, respectively.

Table 1. Some physical data regarding iron (Fe) and zinc (Zc) materials.

Materials	ρ (kg m ⁻³)	E (GPa)	ν
Iron (Fe)	7900	196.2	0.291
Zinc (Zn)	7100	96.4	0.249

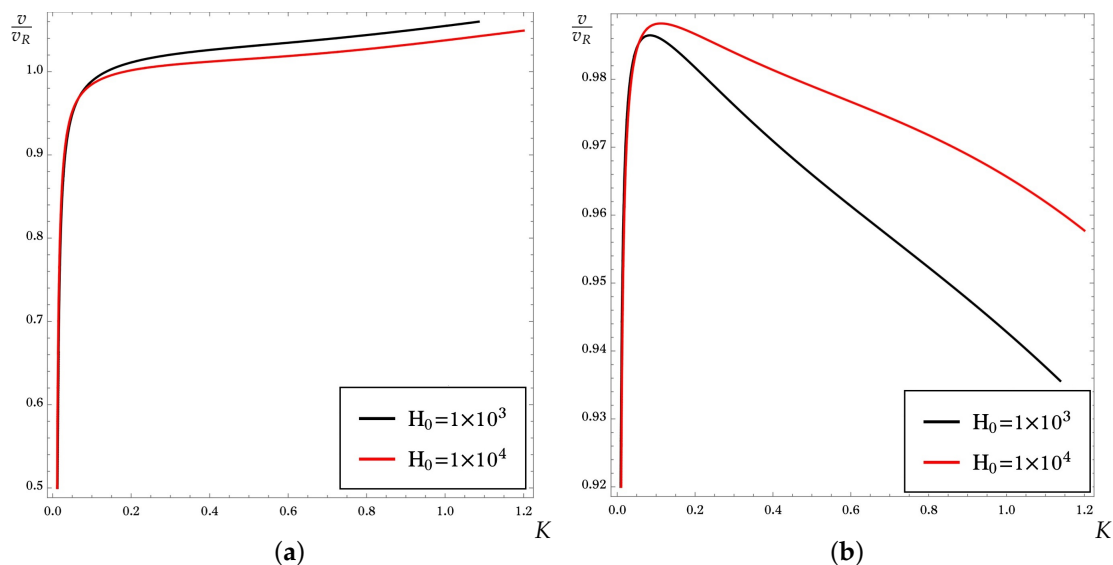


Figure 2. Dependence of the scaled phase velocity $\frac{v}{v_R}$ on the dimensionless wavenumber K with $\zeta = 0.01$. (a) Iron coating and zinc substrate. (b) Zinc coating and iron substrate.

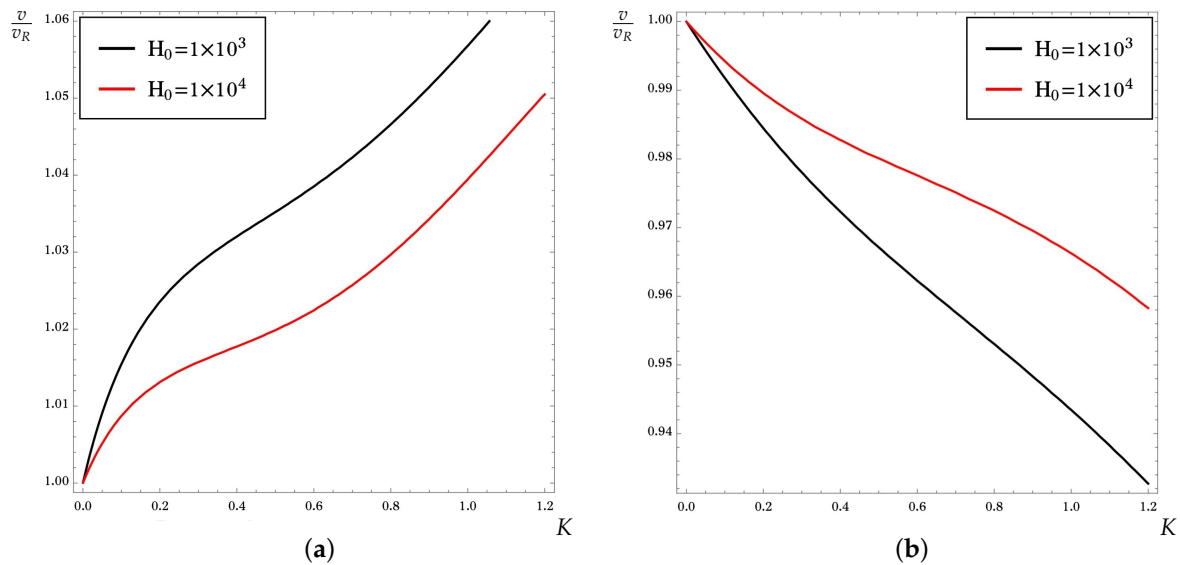


Figure 3. Dependence of the scaled phase velocity $\frac{v}{v_R}$ on the dimensionless wavenumber K with $\zeta = 0$. (a) Iron coating and zinc substrate. (b) Zinc coating and iron substrate.

From these figures, a soft Winkler's elastic foundation [39] is considered in Figure 2 when the dimensionless stiffness of the foundation takes the value $\zeta = 0.01$, for an iron-coated zinc substrate (see Figure 2a), and, on the other hand, for a zinc-coated iron substrate (see Figure 2b), respectively, with the variation in magnetic field intensity H_0 . Similarly, Figure 3 describes the same scenarios as in Figure 2, but with no load; that is, the prescribed normal mechanical load is ignored by setting the dimensionless stiffness of the foundation to be zero, that is when $\zeta = 0$.

In particular, the dependence of the phase speed v/v_R on the dimensionless wavenumber K as shown in Figure 2a for the iron-coated zinc substrate is observed to grow steadily in the same manner, starting around 0.5 to 0.98 on the phase velocity axis, before a sudden steady growth. In fact, an increase in magnetic field intensity H_0 is noted to decrease/reduce the dependency of v/v_R on K . However, in the case of the zinc-coated iron substrate portrayed in Figure 2b, it is equally found to grow steadily in the same manner before a sudden decline. Moreover, the decline is noted to respond more with respect to lesser magnetic field intensity.

Without further delay, Figure 3 maintains a similar trend to that of Figure 2, if not for the absence of the prescribed normal mechanical load, when the dimensionless stiffness of the Winkler's foundation $\zeta = 0$. In fact, the absence of Winkler's foundation widens the independence of v/v_R on K ; at the same time, it maintains the description of the composition of the layers. More clearly, the dependency of the iron-coated zinc substrate starts from 1 on v/v_R axis and increases, while that of the zinc-coated iron substrate decreases from the same point.

5. Asymptotic Solution

The current section is intended to asymptotically study the obtained secular equation in the preceding section. Thus, we begin the section by explaining the basics of the construction of effective boundary conditions for the governing model—the explanation is to be conducted by demonstrating the procedure for the formulated problem. In addition, we would equally establish a comparative study on the two secular equations; the exact versus approximate.

5.1. Treating Coating Layer

Here, we begin by modeling the effect of the homogeneous elastic coating via the effective boundary conditions procedure. Thus, we put into practice in what follows the

direct asymptotic integration of the equations in elasticity, see, e.g., [8,10,11,13,32]. Firstly, let us specify the wavenumber K associated with the long-wave limit, given as

$$K = kh \ll 1. \quad (26)$$

Furthermore, it is appropriate to set the following boundary conditions

$$u_i^c = v_i^s, \quad (27)$$

where $v_i = v_i(x_1, t)$, for $i = 1, 2$ are displacements defined on the interface of the substrate, that is, at $x_2 = 0$.

Next, we introduce the scaling variables

$$\xi = kx_1, \quad \gamma = \frac{x_2}{h} + 1, \quad \tau = kv_{2c}t, \quad (28)$$

along with the following dimensionless quantities

$$u_j^* = ku_j^c, \quad v_j^* = kv_j^s, \quad p^* = \frac{p}{Kk\mu_c}, \quad \sigma_{j2}^* = \frac{\sigma_{j2}^s}{K\mu_c}, \quad \tau_{22}^* = \frac{\tau_{22}^s}{K\mu_c}, \quad j = 1, 2. \quad (29)$$

The equations of motion expressed (5) can then be represented in terms of the new variables as follows

$$\begin{aligned} u_{1,\gamma\gamma}^* + K(\kappa_c^2 - 1)u_{2,\xi\gamma}^* + K^2(\kappa_c^2 u_{1,\xi\xi}^* - u_{1,\tau\tau}^*) &= 0, \\ \kappa_c^2 u_{2,\gamma\gamma}^* + K(\kappa_c^2 - 1)u_{1,\xi\gamma}^* + K^2(u_{2,\xi\xi}^* - u_{2,\tau\tau}^*) &= 0, \end{aligned} \quad (30)$$

together with the new transformed boundary conditions from those prescribed in (19) and (27), given by

$$\begin{aligned} u_{1,\gamma}^* + Ku_{2,\xi}^* &= 0 \quad \text{at} \quad \gamma = -1, \\ \kappa_c^2 u_{2,\gamma}^* + K(\kappa_c^2 - 2)u_{1,\xi}^* &= -K^2 p^* u_2^* \quad \text{at} \quad \gamma = -1, \\ u_j^* &= v_j^* \quad \text{at} \quad \gamma = 0, \end{aligned} \quad (31)$$

where $\kappa_c = v_{1c}/v_{2c}$.

The asymptotic series for the dimensionless displacements may now be written in terms of the small parameter $K \ll 1$ as

$$\begin{pmatrix} u_i^* \\ \sigma_{j2}^* \\ \tau_{22}^* \end{pmatrix} = \begin{pmatrix} u_i^{(0)} \\ \sigma_{j2}^{(0)} \\ \tau_{22}^{(0)} \end{pmatrix} + K \begin{pmatrix} u_i^{(1)} \\ \sigma_{j2}^{(1)} \\ \tau_{22}^{(1)} \end{pmatrix} + K^2 \begin{pmatrix} u_i^{(2)} \\ \sigma_{j2}^{(2)} \\ \tau_{22}^{(2)} \end{pmatrix} + \dots, \quad j = 1, 2. \quad (32)$$

Therefore, upon using (4) and (29)–(32), the stresses σ_{12} and $\sigma_{22} + \tau_{22}$ imply

$$\begin{aligned} K^2 \sigma_{12}^* &= u_{1,\gamma}^{(0)} + K(u_{1,\gamma}^{(1)} + u_{3,\xi}^{(0)}) + K^2(u_{1,\gamma}^{(2)} + u_{2,\xi}^{(1)}) + O(K^3), \\ K^2(\sigma_{22}^* + \tau_{22}^*) &= \kappa_c^2 u_{3,\gamma}^{(0)} + K(\kappa_c^2 u_{3,\gamma}^{(1)} + (\kappa_c^2 - 2)u_{1,\xi}^{(0)}) + K^2(\kappa_c^2 u_{2,\gamma}^{(2)} + (\kappa_c^2 - 2)u_{1,\xi}^{(1)}) + O(K^3). \end{aligned} \quad (33)$$

Then, the solutions for $u_j^{(0)}$, $u_j^{(1)}$, and $u_j^{(2)}$, $j = 1, 2$ are found as follows

$$\begin{aligned} u_j^{(0)} &= v_j^*, & u_1^{(1)} &= -\gamma v_{2,\xi}^*, & u_2^{(1)} &= -\gamma(1 - 2\kappa_c^{-2})v_{1,\xi}^*, \\ u_1^{(2)} &= \gamma \left[\left((-3 + 2\kappa_0^{-2}) \frac{\gamma}{2} - 4(1 - \kappa_c^{-2}) \right) v_{1,\xi\xi}^* + \left(1 + \frac{\gamma}{2} \right) v_{1,\tau\tau}^* \right], \\ u_2^{(2)} &= \gamma \left[(1 - 2\kappa_c^{-2}) \frac{\gamma}{2} v_{2,\xi\xi}^* + \kappa_c^{-2} \left(\left(1 + \frac{\gamma}{2} \right) v_{2,\tau\tau}^* - p^* \right) \right], \end{aligned} \quad (34)$$

such that the stresses expressed in (33) now become

$$\begin{aligned} \sigma_{12}^{(0)} &= (\gamma + 1) \left(v_{1,\tau\tau}^* - 4(1 - \kappa_c^{-2})v_{1,\xi\xi}^* \right) + O(K^2), \\ \sigma_{22}^{(0)} + \tau_{22}^{(0)} &= (\gamma + 1) v_{2,\tau\tau}^* - p^* + O(K^2). \end{aligned} \quad (35)$$

The leading order stresses are then rewritten in terms of the original dimensional variables as

$$\begin{aligned} \sigma_{12}^c(x_1, x_2, t) &= (x_2 + h)\mu_c \left(v_{2c}^{-2} v_{1,tt}^s - 4(1 - \kappa_c^{-2})v_{1,11}^s \right), \\ (\sigma_{22}^c + \tau_{22}^c)(x_1, x_2, t) &= (x_2 + h)\mu_c v_{2c}^{-2} v_{2,tt}^s - p v_2. \end{aligned} \quad (36)$$

Lastly, the effective boundary conditions procedure reveals the following transformed continuity of stresses and displacements at the interface $x_2 = 0$, as follows

$$\begin{aligned} \sigma_{13}^s(x_1, 0, t) &= h\mu_c \left(v_{2c}^{-2} u_{1,tt}^s - 4v_{2c}^2(1 - \kappa_0^{-2})u_{1,11}^s \right), \\ (\sigma_{22}^s + \tau_{22}^s)(x_1, 0, t) &= h\mu_c v_{2c}^{-2} u_{2,tt}^s - p u_2^s. \end{aligned} \quad (37)$$

Note also that these conditions were first presented in [32] for free boundary conditions, using an ad hoc approach, see also [10], cf. (3.17).

5.2. Asymptotic Dispersion Relation

In this subsection, an asymptotic model for surface waves on an elastic half-space (substrate) associated with the effect of normal mechanical load, due to the Winkler's elastic foundation, and that of the magnetic field force will be derived.

Thus, upon following the procedure described in [10,11,13,32], a slow-time perturbation scheme based on the supposition that $K \ll 1$ may be established, revealing the free Rayleigh wave at leading order, with the perturbed wave equation following from the analysis of correction terms. The resulting explicit formulation for surface wave field is expressed in terms of the longitudinal potential ϕ , and non-zero component of the shear potential ψ with the displacement field expressed by using (6). The behavior over the interior of the half-space is governed by the following elliptic equations

$$\phi_{,22}^s + \alpha_R^2 \phi_{,11}^s = 0, \quad \psi_{,22}^s + \beta_R^2 \psi_{,11}^s = 0, \quad (38)$$

where

$$\alpha_R = \sqrt{1 - \frac{v_R^2}{v_{1s}^2}}, \quad \text{and} \quad \beta_R = \sqrt{1 - \frac{v_R^2}{v_{2s}^2}}, \quad (39)$$

with v_R denoting the Rayleigh wave speed.

The boundary condition expressed (38)₁ at $x_2 = 0$ is given by a singularly perturbed wave equation

$$\phi_{,11}^s - \frac{1}{v_R^2} \phi_{,tt}^s - b_1 h \mathcal{H}(\phi_{,111}^s) = -b_2 \frac{p}{\mu_s} \mathcal{H}(\phi_{,1}^s), \quad (40)$$

where \mathcal{H} is Hilbert transform; while b_1 and b_2 are found to be

$$b_1 = \frac{\mu(1 - \beta_R^2)}{2B} \left[\frac{v_R^2}{v_{2c}^2} (\alpha_R + \beta_R) - 4\beta_R (1 - \kappa_c^{-2}) \right], \quad b_2 = \frac{\mu \alpha_R (1 - \beta_R^2)}{2B}, \quad (41)$$

respectively, with

$$B = \frac{\beta_R}{\alpha_R} (1 - \alpha_R^2) + \frac{\alpha_R}{\beta_R} (1 - \beta_R^2) - (1 - \beta_R^4). \quad (42)$$

Obviously, the perturbation terms in (40) are connected with the effect of the coating layer and the Winkler’s foundation can be expressed as a pseudo-differential operator, i.e.,

$$\phi_{,11}^s - \frac{1}{v_R^2} \phi_{,tt}^s - b_1 h \sqrt{-\partial_{,11}} \phi_{,11}^s = -b_2 \frac{p}{\mu_s} \sqrt{-\partial_{,11}} \phi_{,1}^s. \quad (43)$$

Furthermore, the shear potential function ψ^s is found to be

$$\psi^s(x_1 - v_R t, \beta_R x_2) = \frac{1 + \beta_R^2}{2\beta_R} \mathcal{H}(\phi^s(x_1 - v_R t, \beta_R x_2)). \quad (44)$$

The derived equation in (43) leads to the approximation of the exact secular equation earlier determined in (22), as follows

$$\frac{v}{v_R} = \sqrt{1 - \Gamma}, \quad (45)$$

where

$$\Gamma = b_1 K + \frac{b_2 \zeta}{K}. \quad (46)$$

Here, the parameter Γ contains the effect of the coating and the stiffness of the Winkler’s elastic foundation ζ ; we will show later the related relation at which the parameter Γ vanishes.

5.3. Numerical Comparison

This section establishes a comparative analysis graphically. Let us now illustrate graphically the comparison between the obtained approximate secular equation in (45) and that of the exact secular equation earlier determined in (22). Numerical comparison of the exact the secular equation in (22) and that of the asymptotic secular relation in (45) is depicted for $H_0 = 10^3 \text{ kg s}^{-2} \text{ A}^{-1}$ in Figures 4 and 5, sequentially, for $\zeta = 0.01$ and $\zeta = 0$. Furthermore, from these figures, the black solid lines denote the exact dispersion curves of the exact secular equation determined in (22), while the dashed lines correspond to that of the asymptotic secular equation determined in (45).

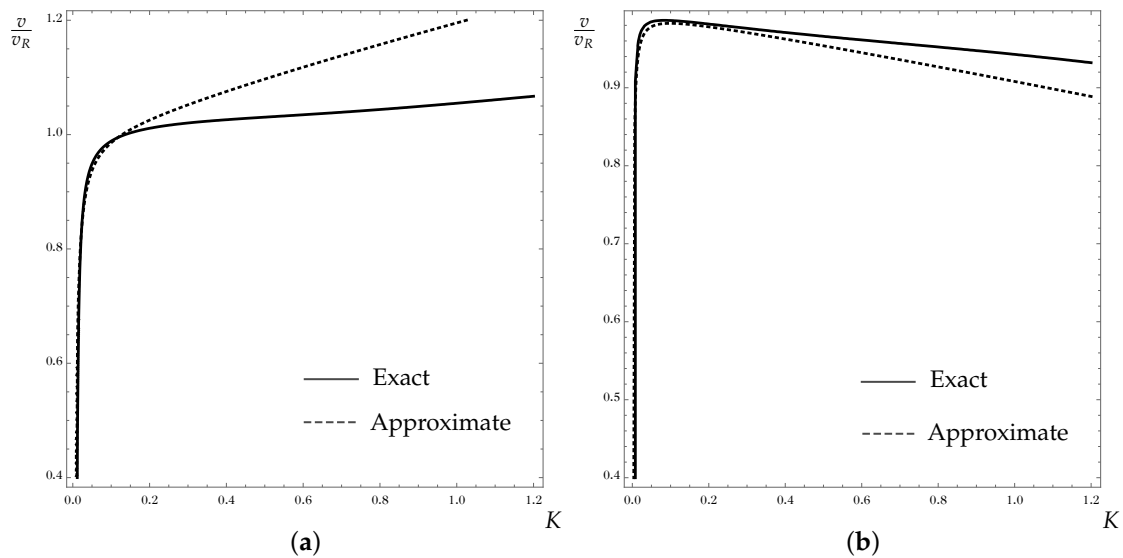


Figure 4. Comparison of the exact (22) and approximate (45) secular equations via the dependence of scaled velocity $\frac{v}{v_R}$ on the dimensionless wavenumber K with $\zeta = 0.01$. (a) Iron coating and zinc substrate. (b) Zinc coating and iron substrate.

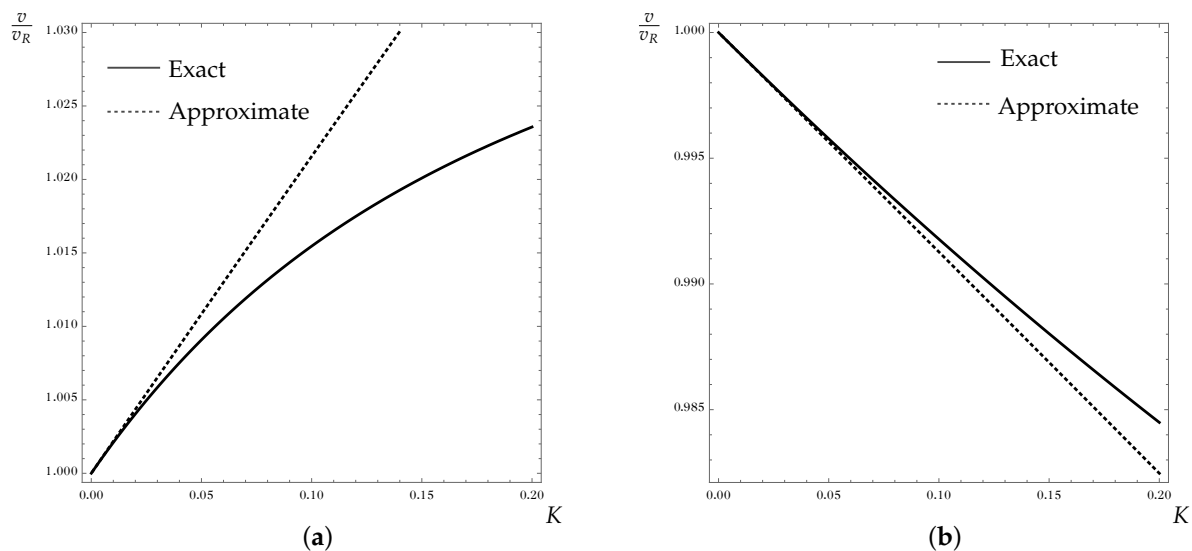


Figure 5. Comparison of the exact (22) and approximate (45) secular equations via the dependence of scaled velocity $\frac{v}{v_R}$ on the dimensionless wavenumber K with $\zeta = 0$. (a) Iron coating and zinc substrate. (b) Zinc coating and iron substrate.

Here, the comparative plots depicted in Figures 4 and 5, respectively, follow the pattern of Figures 2 and 3 with and without the presence of Winkler's elastic foundation—when $\zeta = 0.01$ (a soft elastic foundation) and when $\zeta = 0$. More specifically, a correlation is noted in both Figures 4 and 5 with regard to both the iron-coated zinc substrate (see Figures 4a and 5a), and that of the zinc-coated iron substrate (see Figures 4b and 5b), respectively.

6. Vanishing Possibility of the Coating Layer

In this section, we study the vanishing possibility of the effect of the coating layer through the expression of the constant Γ determined in (45) and (46), that is, when $\Gamma = 0$. As a result, (40) vanishes, and this leads to having only the hyperbolic equation on the surface of a substrate in the case of the absence of the coating layer.

Thus, upon setting $\Gamma = 0$ in (45), the following expression holds

$$E_c = \frac{1}{2(2\beta_R + \zeta_R v_c^-)} \left[2Y \left(v_R^2 \rho_c + v_R^2 \varepsilon_0 H_0^2 \mu_0^2 \right) - 4\beta_R H_0^2 \mu_0 + H_0^2 \mu_0 v_c (4\beta_R - \zeta_R) + H_0^2 \mu_0 \zeta_R \right. \\ \left. - 2v_c^2 \left(v_R^2 \rho_c Y + H_0^2 \mu_0 \left(v_R^2 \varepsilon_0 \mu_0 Y - 4\beta_R + \zeta_R \right) \right) + v_c^+ \left(8Y v_R^2 H_0^2 \mu_0 (1 - 2v_c) \left(\varepsilon_0 H_0^2 \mu_0^2 + \rho_c \right) (2\beta_R + \zeta_R v_c^-) \right. \right. \\ \left. \left. + \left(2\rho_c v_R^2 v_c^- Y + H_0^2 \mu_0 \left(4\beta_R - 8\beta_R v_c + 2v_R^2 \varepsilon_0 \mu_0 v_c^- Y + \zeta_R (2v_c - 1) \right) \right)^2 \right)^{1/2} \right], \quad (47)$$

where

$$v_c^- = v_c - 1, \quad v_c^+ = v_c + 1, \quad Y = \alpha_R + \beta_R, \quad \zeta_R = \frac{\alpha_R \zeta}{K}.$$

From the later equation, we observe that the Young's modulus E_c of the coating layer is non-homogeneously dependent on Winkler's elastic parameter ζ and the dimensionless wavenumber K . Moreover, in the absence of the magnetic field intensity and Winkler's foundation in the equation, that is, when $H_0 = 0$ and $\zeta = 0$, Equation (47) further reduces to the following

$$E_c = \rho_c \left(1 - v_c^2 \right) v_R^2 \left(\frac{\alpha_R^0 + \beta_R^0}{\beta_R^0} \right), \quad (48)$$

where

$$\alpha_R^0 = \sqrt{1 - \frac{v_R^2 (2v_s^2 + v_s - 1) \rho_s}{E_s (v_s - 1)}}, \quad \text{and} \quad \beta_R^0 = \sqrt{1 - \frac{2v_R^2 (v_s + 1) \rho_s}{E_s}}. \quad (49)$$

Numerically, as an example, let us consider an iron substrate (with the following physical data: $E_s = 196.2$ GPa, $v_s = 0.291$, $\rho_s = 7900$ kg m⁻³), with $v_c = 0.249$, $\mu_0 = 4\pi \times 10^{-7}$ kg m s⁻² A⁻², $H_0 = 10^5$ kg s⁻² A⁻¹, and $\varepsilon_0 = 8.85 \times 10^{-12}$ kg⁻¹ m⁻³ s⁴ A². Furthermore, an unloaded case is considered by disregarding Winkler's elastic foundation, by setting the dimensionless stiffness of the foundation to zero, that is, $\zeta = 0$. Thus, the following figures show the vanishing possibility of the effectiveness of the coating layer on the propagation of waves on the governing magneto-elastic coated substrate. Here, the numerical comparison of the exact solution (22) is shown by a solid black line, against the approximate solution (45) that is depicted using the dashed black line.

Figure 6 portrays the occurrences, or rather, the glimpses of the coating's density variation ρ_c through the dependency curves of v/v_R versus K . It can be noted from these Figure 6a–d how possible it is to reduce the effect of the coating layer, by using the values of E_c expressed in (47). Accordingly, we progressively increment the density of the coating layer ρ_c , in such a way that, the density of the half-space substrate ρ_s is approached.

In a nutshell, we conclude that the wider (or closer) the gap between ρ_c and ρ_s , and E_c and E_s , the wider (or closer) the level of exactitude, existing between the approximate and exact dispersion relation, through the dependency curve of v/v_R versus K .

In essence, the effect of the coating layer vanishes steadily when the densities of the coating and that of the substrate are equalized, as correctly captured in Figure 6d. In fact, this scenario somewhat satisfies the instance of a material contrast [43,45].

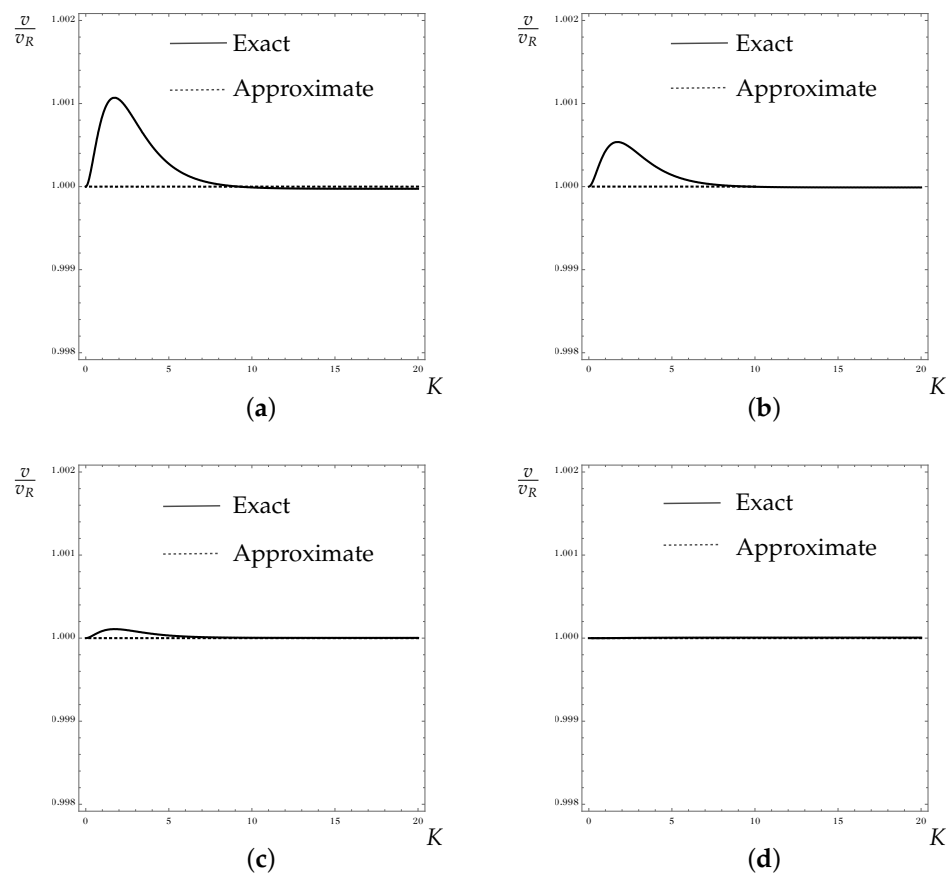


Figure 6. The relationships between $\frac{v}{v_R}$ versus K when the relation (46) is achieved. (a) if $\rho_c = 7800 \text{ kg m}^{-3}$, then $E_c \approx 187.403 \text{ GPa}$. (b) if $\rho_c = 7850 \text{ kg m}^{-3}$, then $E_c \approx 188.611 \text{ GPa}$. (c) if $\rho_c = 7890 \text{ kg m}^{-3}$, then $E_c \approx 189.578 \text{ GPa}$. (d) if $\rho_c = \rho_s = 7900 \text{ kg m}^{-3}$, then $E_c \approx 189.82 \text{ GPa}$.

7. Conclusions

In conclusion, we examined the propagation of plane surface waves on a coated elastic half-space. Sufficient perfect interfacial conditions were prescribed between the coating and the half-space layers. Additionally, owing to the natural incidence of certain external excitations, the structure under deliberation was further exposed to the presence of a magnetic field force, upon which an addition normal mechanical load $P(x_1, t)$ was further prescribed through the application of Winkler's elastic foundation. Moreover, we utilized a couple of analytical and asymptotic integration procedures, thereby acquiring and analyzing the aspiring secular equation. In fact, the influence of the coating layer was suppressed asymptotically by deploying apposite effective boundary conditions. These effective boundary conditions were ingrained in a long-wave approximation condition. Indeed, the comparison between the two approaches yielded a perfect agreement; furthermore, the acquisition of certain well-known results in the literature acted as liming circumstances of the present examination. Additionally, an insightful study about the existence and vanishing possibly of the effectiveness of the coating layer was highlighted graphically and discussed. Lastly, the present study can be used by material scientists, and engineers while designing and constructing multilayered composites—in addition to its huge relevance in the study of seismic waves and earthquakes. More so, a multiply coated heterogeneous structure would be considered a future prospect, with different external forces.

Author Contributions: Conceptualization, A.M.M.; methodology, A.M.M. and F.M.A.; validation, A.M.M. and F.M.A.; formal analysis, A.M.M. and F.M.A.; investigation, A.M.M. and F.M.A.; data curation, A.M.M. and F.M.A.; writing—original draft preparation, A.M.M. and F.M.A.; writing—review and editing, A.M.M. and F.M.A. All authors have read and agreed to the published version of the manuscript.

Funding: This research did not receive any specific external funding other than the funding by Taif University, Taif, Saudi Arabia.

Data Availability Statement: Not applicable.

Acknowledgments: Research support offered by the Deanship of Scientific Research, Taif University, Saudi Arabia [1-442-76] is acknowledged.

Conflicts of Interest: The authors declare no conflict of interest.

References

- Li, M.; Liu, Q.; Jia, Z.; Xu, X.; Cheng, Y.; Zheng, Y.; Wei, S. Graphene oxide/hydroxyapatite composite coatings fabricated by electrophoretic nanotechnology for biological applications. *Carbon* **2014**, *67*, 185–197. [[CrossRef](#)]
- Tiainen, V.M. Amorphous carbon as a bio-mechanical coating-mechanical properties and biological applications. *Diam. Relat. Mater.* **2001**, *10*, 153–160. [[CrossRef](#)]
- Achenbach, J. *Wave Propagation in Elastic Solids*; Elsevier: Amsterdam, The Netherlands, 2012.
- Cho, Y.S. Non-destructive testing of high strength concrete using spectral analysis of surface waves. *NDT E Int.* **2003**, *36*, 229–235. [[CrossRef](#)]
- Krylov, V.V. *Noise and Vibration from High-Speed Trains*; Thomas Telford: Telford, UK, 2001.
- Qian, Z.; Jin, F.; Kishimoto, K.; Wang, Z. Effect of initial stress on the propagation behavior of SH-waves in multilayered piezoelectric composite structures. *Sens. Actuators A Phys.* **2004**, *112*, 368–375. [[CrossRef](#)]
- Palermo, A.; Krodel, S.; Marzani, A.; Daraio, C. Engineered metabarrier as shield from seismic surface waves. *Sci. Rep.* **2016**, *6*, 39356. [[CrossRef](#)]
- Kaplunov, J.; Prikazchikov, D.; Sultanova, L. Rayleigh-type waves on a coated elastic half-space with a clamped surface. *Philos. Trans. R. Soc. A* **2019**, *377*, 20190111. [[CrossRef](#)]
- Vinh, P.C.; Anh, V.T.N.; Thanh, V.P. Rayleigh waves in an isotropic elastic half-space coated by a thin isotropic elastic layer with smooth contact. *Wave Motion* **2014**, *51*, 496–504. [[CrossRef](#)]
- Dai, H.H.; Kaplunov, J.; Prikazchikov, D.A. A long-wave model for the surface elastic wave in a coated half-space. *Proc. R. Soc. A* **2010**, *466*, 3097–3116. [[CrossRef](#)]
- Mubaraki, A.M.; Helmi, M.M.; Nuruddeen, R.I. Surface wave propagation in a rotating doubly coated nonhomogeneous half space with application. *Symmetry* **2022**, *14*, 1000. [[CrossRef](#)]
- Mubaraki, A.; Althobaiti, S.; Nuruddeen, R.I. Propagation of surface waves in a rotating coated viscoelastic half-space under the influence of magnetic field and gravitational forces. *Fractal Fract.* **2021**, *5*, 250. [[CrossRef](#)]
- Mubaraki, A.; Prikazchikov, D.; Kudaibergenov, A. Explicit model for surface waves on an elastic half-space coated by a thin vertically inhomogeneous layer. In *Dynamical Systems Theory and Applications*; Springer: Cham, Switzerland, 2019; pp. 267–275.
- Mubariki, A.; Prikazchikov, D. On Rayleigh wave field induced by surface stresses under the effect of gravity. *Math. Mech. Solids* **2020**, *27*, 1771–1782. [[CrossRef](#)]
- Abo-Dahab, S.M.; Lotfy, K.; Gohaly, K.A. Rotation and magnetic field effect on surface waves propagation in an elastic layer lying over a generalized thermoelastic diffusive half-space with imperfect boundary. *Math. Probl. Eng.* **2015**, *2015*, 671783. [[CrossRef](#)]
- Abd-Alla, A.M.; Abo-Dahab, S.M.; Khan, A. Rotational effects on magneto-thermoelastic Stoneley, Love, and Rayleigh waves in fibre-reinforced anisotropic general viscoelastic media of higher order. *Comput. Mater. Contin.* **2017**, *53*, 49–72.
- Selim, M.M. Effect of thermal stress and magnetic field on propagation of transverse wave in an anisotropic incompressible dissipative initially stressed plate. *Appl. Math. Inf. Sci.* **2017**, *11*, 195–200. [[CrossRef](#)]
- Nuruddeen, R.I.; Nawaz, R.; Zia, Q.M.Z. Investigating the viscous damping effects on the propagation of Rayleigh waves in a three-layered inhomogeneous plate. *Phys. Scr.* **2020**, *95*, 065224. [[CrossRef](#)]
- Wang, Y.Z.; Li, F.M.; Kishimoto, K. Thermal effects on vibration properties of double-layered nanoplates at small scales. *Compos. Part B Eng.* **2011**, *42*, 1311–1317. [[CrossRef](#)]
- Yu, J.; Ma, Q.; Su, S. Wave propagation in non-homogeneous magneto-electro-elastic hollow cylinders. *Ultras* **2008**, *48*, 664–677. [[CrossRef](#)]
- Asif, M.; Nawaz, R.; Nuruddeen, R.I. Dispersion of elastic waves in an inhomogeneous multilayered plate over a Winkler elastic foundation with imperfect interfacial conditions. *Phys. Scr.* **2021**, *96*, 125026. [[CrossRef](#)]
- Slepyan, L.I. *Models and Phenomena in Fracture Mechanics*; Springer Science & Business Media: Berlin/Heidelberg, Germany, 2012.
- Ahmad, F.; Zaman, F.D. Exact and asymptotic solutions of the elastic wave propagation problem in a rod. *Int. J. Pure Appl. Math.* **2006**, *27*, 123–127.
- Alzaidi, A.S.M.; Mubaraki, A.M.; Nuruddeen, R.I. Effect of fractional temporal variation on the vibration of waves on elastic substrates with spatial non-homogeneity. *AIMS Math.* **2022**, *7*, 13746–13762. [[CrossRef](#)]
- Biot, M.A. Thermoelasticity and irreversible thermodynamics. *J. Appl. Phys.* **1956**, *27*, 240253. [[CrossRef](#)]
- Chandrasekharai, D.S. Thermoelasticity with second sound: A review. *Appl. Mech. Rev.* **1986**, *39*, 355–376. [[CrossRef](#)]
- Lord, H.W.; Shulman, Y. A generalized dynamical theory of thermoelasticity. *J. Mech. Phys. Solids* **1967**, *15*, 299–309. [[CrossRef](#)]
- Green, A.E.; Naghdi, P.M. Thermoelasticity without energy dissipation. *J. Elast.* **1993**, *31*, 189–208. [[CrossRef](#)]

29. Chandrasekharai, D.S. Hyperbolic thermoelasticity: A review of recent literature. *Appl. Mech. Rev.* **1998**, *51*, 705–729. [[CrossRef](#)]
30. Althobaiti, S.; Mubarak, A.; Nuruddeen, R.I.; Gomez-Aguilar, J.F. Wave propagation in an elastic coaxial hollow cylinder when exposed to thermal heating and external load. *Results Phys.* **2022**, *38*, 105582. [[CrossRef](#)]
31. Mubarak, A.M.; Althobaiti, S.; Nuruddeen, R.I. Heat and wave interactions in a thermoelastic coaxial solid cylinder driven by laser heating sources. *Case Stud. Therm. Eng.* **2022**, *38*, 102338. [[CrossRef](#)]
32. Kaplunov, J.; Prikazchikov, D.A. Asymptotic theory for Rayleigh and Rayleigh-type waves. *Adv. Appl. Mech.* **2017**, *50*, 1–106. [[CrossRef](#)]
33. Kaplunov, J.; Kossovich, L.Y.; Nolde, E.V. *Dynamics of Thin Walled Elastic Bodies*; Academic Press: San Diego, CA, USA, 1998.
34. Goldenveizer, A.L. Asymptotic method in the theory of shells. *Theor. Appl. Mech.* **1980**, 91–104.
35. Tiersten, H.F. Elastic surface waves guided by thin films. *J. Appl. Phys.* **1969**, *40*, 770–789. [[CrossRef](#)]
36. Nolde, E.V.; Rogerson, G.A. Long wave asymptotic integration of the governing equations for a pre-stressed incompressible elastic layer with fixed faces. *Wave Motion* **2002**, *36*, 287–304. [[CrossRef](#)]
37. Kaplunov, J.; Kossovich, L.Y. Asymptotic model of Rayleigh waves in the far-field zone in an elastic half-plane. *Dokl. Phys.* **2004**, *49*, 234–236. [[CrossRef](#)]
38. Kuznetsov, V.I. *Elastic Foundations*; Gosstroizdat: Moscow, Russia, 1952.
39. Erbas, B.; Kaplunov, J.; Nobili, A.; Kilic, G. Dispersion of elastic waves in a layer interacting with a Winkler foundation. *J. Acoust. Soc. Am.* **2018**, *144*, 2918–2925. [[CrossRef](#)]
40. Kaplunov, J.; Prikazchikov, D.; Prikazchikova, L. Dispersion of elastic waves in a strongly inhomogeneous three-layered plate. *Int. J. Solids Struct.* **2017**, *113*, 169–179. [[CrossRef](#)]
41. Anya, A.I.; Akhtar, M.W.; Abo-Dahab, S.M.; Kaneez, H.; Khan, A.; Jahangir, A. Effects of a magnetic field and initial stress on reflection of SV-waves at a free surface with voids under gravity. *J. Mech. Behav. Mater.* **2018**, *27*, 20180002. [[CrossRef](#)]
42. Poisson Ratios. Available online: <http://matweb.com> (accessed on 1 October 2022).
43. Prikazchikov, L.A.; Aydin, Y.E.; Erbas, B.; Kaplunov, J. Asymptotic analysis of anti-plane dynamic problem for a three-layered strongly inhomogeneous laminate. *Math. Mech. Solids* **2018**, *56*, 189. [[CrossRef](#)]
44. Ross, R.B. *Metallic Materials Specification Handbook*, 3rd ed.; Springer: London, UK, 1980.
45. Kaplunov, J.; Prikazchikov, D.A.; Prikazchikov, L.A.; Sergushova, O. The lowest vibration spectra of multi-component structures with contrast material properties. *J. Sound Vib.* **2019**, *445*, 132–147. [[CrossRef](#)]